

# Synthesis, optical properties and modeling of silver core–silver oxide shell nanostructures in silica films

Víctor M. Rentería–Tapia<sup>1</sup>, Guadalupe Valverde–Aguilar<sup>1</sup>, Jorge A. García–Macedo<sup>1</sup>

1. Instituto de Física, Universidad Nacional Autónoma de México. Circuito exterior 04510. Cd. Universitaria Coyoacán. México D.F. Phone: (5255) 56225103, FAX: (5255) 56161535.

## ABSTRACT

Sol–gel silica films containing silver ions were annealed in a rich–hydrogen atmosphere and subsequently in a rich–oxygen atmosphere. High resolution transmission electronic microscopy measurements shown unusual core–shell structures of silver–silver oxide nanoparticles in these films. The optical properties of these nanostructures exhibited red shift and damping in the UV–vis spectra. In order to calculate the optical properties were used the Mie theory using two approaches. The first one, corresponding to the core–shell model that includes a refractive index of the shell ( $n_s$ ) different to the one of the host matrix ( $n_m$ ). While in the second approach, we replaced in the Mie theory the refractive index of the environment (silica) by a local refractive index ( $n_l$ ) depending on the thickness of the silver oxide shell. Both calculations given the same results because they are equivalents.

Keywords: Nanostructures; Thin films; Optical properties; Surface plasmon resonance; Silver nanoparticles; Silver oxide; Mie Theory.

### \* Contact author:

Dr. Jorge Garcia Macedo  
Instituto de Física, UNAM  
PO Box 20–364, 01000  
México, D.F.  
México.  
Tel. (52) 5–622–51–03  
Fax (52) 5–616–15–35  
E–mail [gamaj@fisica.unam.mx](mailto:gamaj@fisica.unam.mx)

## 1. INTRODUCTION

The influence of oxidizing atmospheres plays a very important role on the catalytic, electric, magnetic and optical properties of metallic nanoparticles as function of the temperature.<sup>1–4</sup> This is because the interaction of the metallic nanoparticles with oxygen could lead to metallic core–metallic oxide shell structures<sup>2–4</sup> or complete metallic oxidation under oxidizing atmosphere.<sup>5</sup> Specifically, silver nanoparticles in silica films prepared by the sol–gel method decrease in size and undergo complete oxidation while being heat–treated in an air atmosphere.<sup>6–7</sup> Despite the oxidation of metallic nanoparticles notably affect their properties, this surface effect is usually underestimated in the experimental measurements or theoretical models. So that, the purpose of our work is the synthesis of unusual silver core–silver oxide shell nanostructures in sol–gel silica films, their optical characterization and modeling.

## 2. EXPERIMENTAL

The samples were prepared with Tetraethoxyorthosilicate (TEOS) and silver nitrate ( $\text{AgNO}_3$ ) from Aldrich, ethanol (EtOH) from Merck and distilled water. The reactants were mixed in the relative molar concentrations  $\text{TEOS}/\text{H}_2\text{O}/\text{EtOH}/\text{AgNO}_3 = 1/4/3/0.017$ . Under strong stirring, concentrated nitric acid was added in the solution until the pH was around 1.5. Subsequently, the sol was deposited on silica glass substrates by the dip-coating method at 5 cm/min, obtaining a homogeneous layer. Initially, the silica films were put in a cylindrical oven and heated at 550 °C for 20 hours in air atmosphere to remove the organic part from the composites.<sup>8</sup> Afterwards, the films were heated in a rich-hydrogen atmosphere at 430 °C from 0 to 18 minutes and subsequently were heated from 0 up to 60 minutes at the same temperature in a rich-oxygen atmosphere. In all cases, the samples were quenched in air by dropping the sample on a copper plate. The optical properties of the films were recorded with a Thermospectronic Genesys 2 spectrophotometer at room temperature. The transmission electronic microscopy (TEM) and high resolution transmission electron microscopy (HRTEM) analysis were performed in a JEM-2010F FasTEM field-emission transmission electron microscope with an accelerating voltage of 200 kV and with a resolution point to point of 0.19 nm. The samples were prepared using carbon-coated copper grids of 3 mm in diameter.

## 3. RESULTS

The optical spectra of nanoparticles obtained at 430 °C for 18 minutes in hydrogen atmosphere and subsequently heated for 60 minutes in an oxygen atmosphere are shown in Fig. 1. In Fig. 1a, it is observed a selective absorption due to silver nanoparticles<sup>9</sup> obtained by the reduction of the silver ions in hydrogen atmosphere. This optical spectrum has a full-width at half maximum (FWHM) of the absorption peak of 51 nm and their maximum is located at 398 nm. However, for samples heated in an oxygen atmosphere the optical spectrum is damped and exhibits a red shift (Fig. 1b) as compared with the spectrum in Fig. 1a. According to Fig. 1b, the FWHM is 66 nm, their maximum wavelength is located in 408 nm and the optical absorption band diminished 50%.

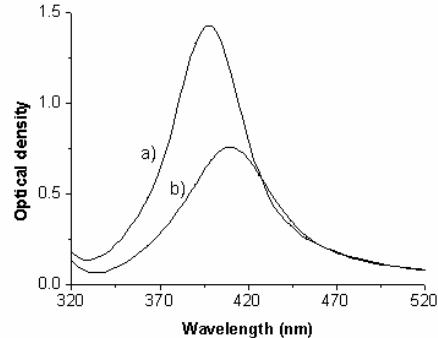


Fig.1. Absorption spectra of silver nanoparticles in silica films annealed at 430 °C in a) a hydrogen atmosphere for 18 min and b) an oxygen atmosphere for 60 min.

Fig. 2 shows the evolution of the maximum absorption of the silver nanoparticles as function heating time in reducing and oxidizing atmosphere at 430 °C. At the beginning of the reduction the absorption peak is located at 400 nm and was blue shift (2nm) to the final of this heat treatment (Fig. 2a). However, an important red shift is observed for silver nanoparticles in an oxygen atmosphere as function heating time (Fig. 2b). At short heating times the effect is more pronounced than at longer heating times. In fact, after 20 minutes of heating the maximum absorption located at 408 nm is practically the same. The optical absorption was also gradually damped during heat treatment in an oxygen atmosphere. Nevertheless, the intensity of the spectrum and the position of the maximum peak did not change for longer time (at least one year) at room temperature, suggesting that the morphology of the silver nanoparticles was stable during this time.

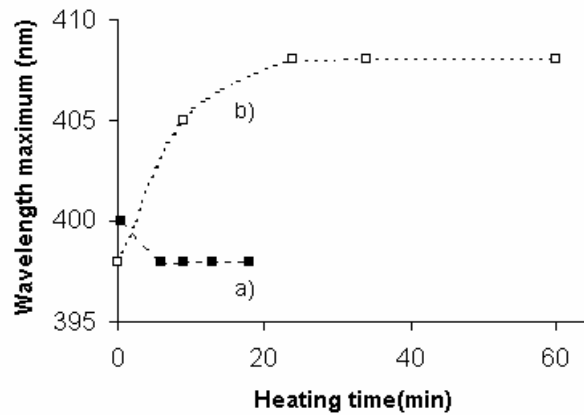


Fig. 2. Evolution of the maximum wavelength of silver nanoparticles annealed at 430 °C in a) reducing atmosphere and b) oxidizing atmosphere.

#### 4. DISCUSSION

The damping and red shift of the optical absorption observed in Fig. 1b, suggest an oxidation process of small silver nanoparticles after heating in rich-oxygen atmosphere. In order to confirm this asseveration, we obtained TEM and HRTEM images of the silver nanoparticles in the silica films heated at 430 °C by 60 min under oxidizing atmosphere (Fig. 3). In Fig. 3a, we predominantly observed small silver nanoparticles (2R~7 nm) with almost spherical shape and well-separated, although there was also a small amount of big nanoparticles (2R~24 nm). Apparently, the image shows typical silver nanoparticles in the silica films. However, enlarged HRTEM images of some silver nanoparticles shown core-shell structures. For example, in Fig. 3b we can observe a core of ~14 nm of size and a shell of ~2 nm of thickness. The filtered HRTEM image clearly showed the presence of a silver core and a silver oxide shell. Nevertheless, it is important mention that for small silver nanoparticles (diameter  $\leq 7$  nm) was very difficult to observe these silver oxide shells.

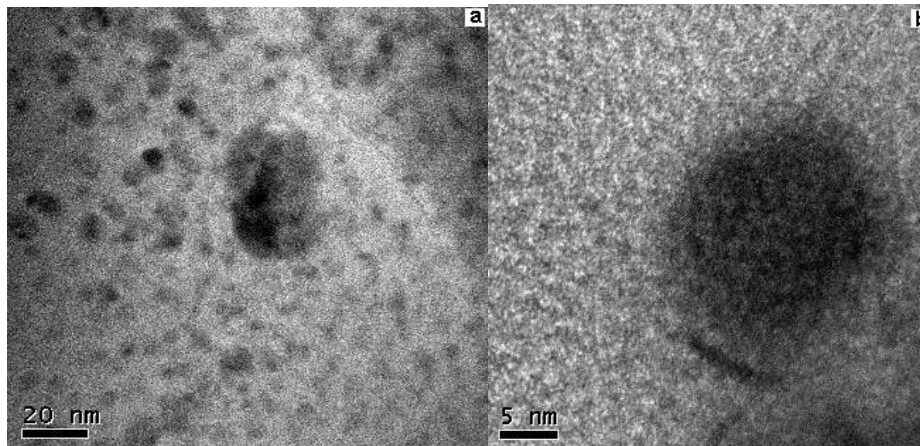


Fig. 3. a) TEM image of silver nanoparticles oxidizing in an oxygen atmosphere. b) Enlarged image of a core silver-silver oxide shell nanostructure.

In agreement with this last result, very thin shells are predicted for small radii  $R$  of metallic core according to the next equation,<sup>10</sup>

$$d = R \left( \frac{1}{\sqrt[3]{1-g}} - 1 \right) \quad (1)$$

Where  $d$  is the thickness of the shell and  $g$  its volume fraction. In Fig. 4 is shown this relationship with a best detail. According with this figure, we can observe only considerable thickness of the shell for small nanoparticles with very high values of the volume fraction  $g$  or for very big particles with high value of  $g$ . In our samples, the second case certainly was easily observed. So, the relationship observed in Fig. 4 explain the large difficult to identify thin silver oxide shells on the surface of small core silver nanoparticles, and therefore why they are not usually detected .

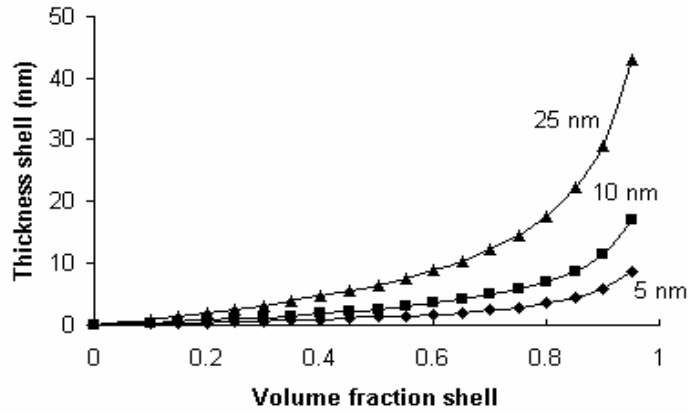


Fig 4. Relationship between the thickness shell and the volume fraction of silver oxide shells for several radii size of core particles.

On the other hand, in order to calculate the optical absorption of these nanostructures we used the core-shell model.<sup>11</sup> In this model based on the Mie theory is included the influence of the complex dielectric function of the shell on the core polarization charge which determined the maximum wavelength and damping changes.<sup>10,11</sup>

For core spherical particles covered with a concentric spherical shell the absorption coefficient  $\alpha$  is given thus;<sup>11</sup>

$$\alpha = \frac{6\pi\phi\sqrt{\epsilon_m}}{\lambda} \text{Im} \left\{ \frac{(\epsilon_s - \epsilon_m)(\epsilon_c - 2\epsilon_s) + (1-g)(\epsilon_c - \epsilon_s)(\epsilon_m + 2\epsilon_s)}{(\epsilon_s + 2\epsilon_m)(\epsilon_c + 2\epsilon_s) + (1-g)(2\epsilon_s - 2\epsilon_m)(\epsilon_c - \epsilon_s)} \right\} \quad (2)$$

$\phi = 1-g$  is the volume fraction of the metal,  $g$  is the volume fraction of the shell layer,  $\epsilon_m = n_m^2$  is the dielectric constant of the surrounding medium,  $\epsilon_c$  and  $\epsilon_s = n_s^2$ , are the complex dielectric function of the core material and that of the shell, respectively. In the limit case when  $g = 0$ , the eq. 2 gives the Mie theory for spherical particles without shell and when  $g = 1$  gives the optical absorption spectrum for a sphere of the shell material. The origin of the color of the films with small silver nanoparticles is explained when the denominator in eq. 2 fulfilled the resonance condition.<sup>10</sup> The result of this condition is the selective absorption observed in the optical spectra, named surface plasmon resonance. On the other hand, according to the classical calculations for nanoparticles within 3–20 nm diameter size range there is not a strong dependence of the particle size on the absorption peaks.<sup>12</sup> However, the optical absorption band is broadened, blue shift and intensity decreased with reduction of the particle size (below 3 nm diameter size), due to the modification of the mean-free path of the conduction electrons. So that, in this case  $\epsilon_c(\omega, R) = \epsilon_1(\omega, R) + i\epsilon_2(\omega, R)$  is depending on the frequency  $\omega$  and of the radius  $R$  of the core and is given as follow:<sup>13</sup>

$$\epsilon_2(\omega, R) = \epsilon_2(\omega) + \eta \frac{\omega_p^2}{\omega^3} \left( \frac{V_f}{R} \right) \quad (3)$$

where  $\omega_p$  is the plasma frequency ( $1.38 \times 10^{16} \text{ s}^{-1}$ ),  $V_f$  is the Fermi velocity of the conduction electrons ( $1.4 \times 10^6 \text{ ms}^{-1}$ ),  $\eta$  is a factor that is relating with the scattering rate of the free electrons against other electrons, the particle surface, phonons, defects and so on.<sup>13-14</sup> Thus, this factor is a consequence of the limitation of the electron motion and generally their value is  $\eta \approx 1$ .<sup>14</sup> On the other hand, the surface plasmon peak position of metal core-shell nanostructures is calculated by<sup>10</sup>

$$\frac{\omega_p^2}{\omega^2} = \epsilon^\infty + 2\epsilon_m + \frac{2g(\epsilon_s - \epsilon_m)}{3} \quad (4)$$

Where  $\epsilon^\infty$  is the high frequency dielectric constant due to interband and core transitions.<sup>11</sup> The eq. 4 gives practically the same result that to naked particles provided that  $g \rightarrow 0$  (thin shell). Likewise, the expression corresponding to  $\epsilon_2(\omega, R)$  in eq. 3 should be modified in order to take into account the influence of the frequency on the variations in the thickness of the shell via the  $g$  factor (eq. 4). Nevertheless, as note above the influence of a thin silver oxide shell on the dielectric constant  $\epsilon_2$  can be underestimated when  $g \rightarrow 0$ . Taking into account these considerations, Fig. 5 shows the fits calculated by the core-shell model to the experimental spectra obtained in reducing and oxidizing atmosphere at  $430^\circ\text{C}$ . In all fits we used  $\eta = 1$ ,  $\epsilon_s = 6.25$ ,  $\epsilon_m = 2.13$  and  $R$  and  $g$  were free parameters.<sup>14,15</sup> The dielectric data  $\epsilon_1$  and  $\epsilon_2$  were obtained from Johnson and Christy.<sup>16</sup> In Fig. 5a is shown the best fit for the spectrum of silver nanoparticles obtained in reducing atmosphere. The calculations predicted silver spherical nanoparticles of radius  $2R = 4.8 \text{ nm}$  and  $g = 0$ . Despite we were used free parameters in this fit, the area under the experimental curve was not totally fill for the calculated curve. This is probably due to the distribution of the shape and size of the metallic nanoparticles were not totally homogeneous (Fig. 3a). On the other hand, in Fig. 5b is shown the best fit for the spectrum of silver nanoparticles obtained in an oxygen atmosphere. The calculations done to this experimental spectrum given  $2R = 4.2 \text{ nm}$  and  $g = 0.15$ . The difference of area observed between the experimental and calculated spectra in Fig. 5b, is due to the same explanation given above. Although, we should also note that it is necessary to include a detail distribution of the size and shape of the metallic nanoparticles in the calculations. So that, the calculated spectrum allows us estimate the volume fraction  $g$  of the shell, their thickness or inclusive predict the oxidation state on the surface of the metallic nanoparticles.

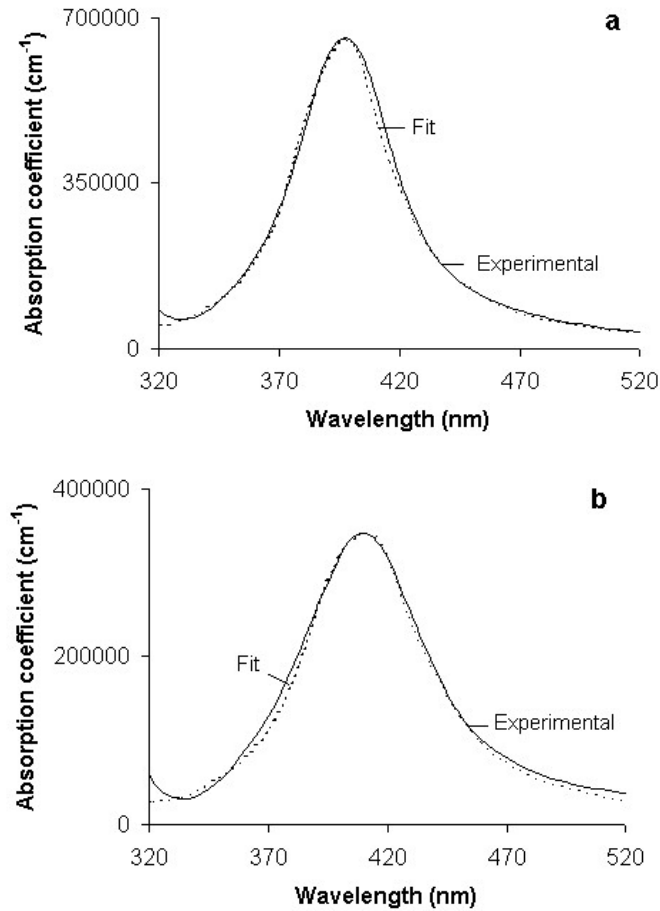


Figure 5. Core-shell theory fit (dashed line) of the optical absorption spectrum for a sample annealed at 430 °C in a) reducing atmosphere and b) in oxidizing atmosphere.

The calculations done with the core-shell model shown that the size and shape of the silver nanoparticles practically remain constant after heat treatment under reducing and oxidizing atmosphere, respectively. However, the surface of the silver nanoparticles reacts with oxygen given a thin silver oxide shell around them, which thickness grows with the oxidation process and it will determinate the wavelength of the optical band as well as the damping. After saturation, the silver oxide acts as a protective shell that stabilizes the metallic nanoparticles, similarly to silver-silver oxide shell nanostructures in silica gels.<sup>15</sup>

Unfortunately, because it is not easy get experimental data of the complex dielectric function of the shell, it is necessary to consider another possibilities that allow us to predict the important parameters in the core-shell structures without use those function. Recently, an alternative to this problem was proposed that is based on the inclusion of a local refractive index in the Gans theory.<sup>15</sup> This theory is an extension of the Mie theory for prolate particles and the refractive index of the surrounding medium is replaced by a variable refractive index due to silver oxide shells of several thickness. So, using this approach,  $n_m$  becomes in a local refractive index  $n_1$  in the eq. 2 provided that  $\epsilon_m = \epsilon_s = n_1^2$ . Physically, that means that the optical properties of the silver nanoparticles are not notably affected by the dielectric constant coming from the host matrix otherwise their properties were predominantly affected by the  $n_1$  value coming from silver oxide shells of different thickness. The  $n_1$  value is depending on the experimental maximum wavelength and consequently of the thickness of the shell.<sup>15</sup> So that, if we taken into account this second approach we obtained a very good fit (not shown) with  $n_1 = 1.58$  and  $2R = 4.3$  nm, for the spectrum observed in Fig. 1b. The traditional core-shell model and the Mie theory including a local refractive index given similar results, because both approaches are equivalents.<sup>15</sup>

## 5. CONCLUSIONS

Silver core–silver oxide shell nanostructures in sol–gel silica films were obtained at 430 °C in a reducing and subsequently in an oxidizing atmosphere. However, the shells of the silver oxide are easily observed in big particles than for small nanoparticles in agreement with predictions done by the theory. The experimental spectra were calculated by the Mie theory using two methods. We achieved very good fits in both cases due to equivalence between these methods. The contributions of silver core–silver oxide shell species are very important on the optical properties of the films.

## 6. ACKNOWLEDGMENTS

+ With economical support from Conacyt. Work supported by Conacyt (México), Project 43226 and PAPIIT UNAM IN 116506. We also thank the technical assistance from Luis Rendón and Edilberto Hernandez.

## 7. REFERENCES

- (1) Z. Qu, M. Cheng, X. Dong and X. Bao, “CO selective oxidation in H<sub>2</sub>-rich gas over Ag nanoparticles—effect of oxygen treatment temperature on the activity of silver particles mechanically mixed with SiO<sub>2</sub>”, *Catal. Today*, **93**, 247, (2004).
- (2) D. Chakravorty, S. Basu, P.K. Mukherjee, S.K. Saha, B.N. Pal, A. Dan and S. Bhattacharya, “Novel properties of glass–metal nanocomposites”, *J. Non–Cryst. Solids*, **352**, 601, (2006).
- (3) L.C. Varanda, M.P. Morales, G.F. Goya, M. Imaizumi, C.J. Serna and Jr. M. Jafelicci, “Magnetic properties of acicular Fe<sub>1-x</sub>RE<sub>x</sub> (RE = Nd, Sm, Eu, Tb; x = 0, 0.05, 0.10) metallic nanoparticles”, *Mater. Sci. Eng. B*, **112**, 188, (2004).
- (4) S. Basu and D. Chakravorty, “Optical properties of nanocomposites with iron core–iron oxide shell structure”, *J. Non–Cryst. Solids* **352**, 380, (2006).
- (5) M. Lyubovsky and L. Pfefferle, “Complete methane oxidation over Pd catalyst supported on  $\alpha$ -alumina. Influence of temperature and oxygen pressure on the catalyst activity”, *Catal. Today*, **47**, 29, (1999).
- (6) M. Mennig, M. Schmitt and H. Schmidt, “Synthesis of Ag-colloids in sol-gel derived SiO<sub>2</sub>-coatings on glass”, *J. Sol–gel Sci. Technol.*, **8**, 1035, (1997).
- (7) W. Li, S. Seal, E. Megan, J. Ramsdell, K. Scammon, G. Lelong, L. Lachal and K.A. Richardson, “Physical and optical properties of sol-gel nano-silver doped silica film on glass substrate as a function of heat-treatment temperature”, *J. Appl. Phys.*, **93**, 9553, (2003).
- (8) G. Mitrikas, C.C. Trapalis, N. Boukos, V. Psyharis, L. Astrakas and G. Kordas, “Size distribution and EPR of silver nanoparticles in SiO<sub>2</sub> matrix”, *J. Non–Cryst. Solids*, **224**, 17, (1998).
- (9) R.H. Doremus, “Optical properties of small silver particles”, *J. Chem. Phys.*, **42**, 414, (1964).
- (10) A.C. Templeton, J. J. Pietron, R. W. Murray and P. Mulvaney, “Solvent refractive index and core charge influences on the surface plasmon absorbance of alkanethiolate monolayer-protected gold clusters”, *J. Phys. Chem. B.*, **104**, 564, (2000).
- (11) P. Mulvaney, “Surface plasmon spectroscopy of nanosized metal particles”, *Langmuir*, **12**, 788, (1996).
- (12) J.A. Creighton and D.G. Eadon, “Ultraviolet–visible absorption spectra of the colloidal metallic elements”, *J. Chem. Soc. Faraday Trans.*, **87**, 3881, (1991).
- (13) P.J. Hull, J.L. Hutchison, O.V. Salata and P.J. Dobson, “Synthesis of nanometer–scale silver crystallites via a room–temperature electrostatic spraying process”, *Adv. Mat.*, **9**, 413, (1997).
- (14) C. Voisin, N. Del Fatti, D. Christofilos and F. Vallee, “Ultrafast electron dynamics and optical nonlinearities in metal nanoparticles”, *J. Phys. Chem. B.*, **105**, 2264, (2001).
- (15) V.M. Rentería and J. García–Macedo, “Modeling of optical absorption of silver prolate nanoparticles embedded in sol–gel glasses”, *Mater. Chem. Phys.*, **91**, 88, (2005).
- (16) P.B. Johnson and R.W. Christy, “Optical constants of the noble metals”, *Phys. Rev. B*, **6**, 4370, (1972).